Enhanced Monopulse Radar Tracking Using Empirical Mode Decomposition

Sherif A. Elgamel[#1], John J. Soraghan[#2]

[#] Department of Electronic and Electrical Engineering University of Strathclyde
Glasgow, UK
[1] sherifelgamel73@gmail.com
[2] j.soraghan@eee.strath.ac.uk

Abstract— **Monopulse radar processors are used to track targets that appear in the look direction beamwidth. The target tracking information (range, azimuth angle, and elevation angle) are affected when manmade high power interference (jamming) is introduced to the radar processor through the radar antenna main lobe (main lobe interference) or antenna side lobe (side lobe interference). This interference changes the values of the error voltage which is responsible for directing the radar antenna towards the target. A monopulse radar structure that uses filtering in the empirical mode decomposition (EMD) domain is presented in this paper. EMD is carried out for the complex radar chirp signal with subsequent denoising and thresholding processes used to decrease the noise level in the radar processed data. The performance enhancement of the monopulse radar tracking system with EMD based filtering is included using the standard deviation angle estimation error (STDAE) for different jamming scenarios and different target SNRs.**

I. INTRODUCTION

Monopulse radars are commonly used in target tracking because of their angular accuracy. However, these radars are affected by different types of interference which affects the target tracking process and may lead to inaccurate tracking [1]. A high power interference (jamming) may be introduced to the radar processor through the radar antenna main lobe (main lobe interference) or antenna side lobe (side lobe interference). The resultant distortion due to this interference will affect the induced target error voltage and consequently the radar tracking ability. Seliktar et al. [2] suggests adding constraints to the monopulse processors steering vectors to decrease the effect of the noise interference before extracting the target information. In our work the radar signal is processed in the empirical mode decomposition (EMD) domain to reduce the interference noise before supplying the received radar data to the monopulse processor.

EMD based real signal denoising is described in [3] and [4]. In our work we propose the use of an EMD filter to cancel interference signal that appears in the main beam look direction without adding any more constraints to the monopulse processor. Following a brief introduction to the empirical mode decomposition (EMD) the paper will describe the structure of the new EMD based monopulse radar processor. The superior performance of the new monopulse algorithm will be demonstrated for different jamming scenarios.

II. MONOPULSE RADAR PROCESSORS

A. Monopulse Radar Processors

1) The conventional processor is a non adaptive configuration comprising two sets of weights set to the sum and difference steering vectors. These steering vectors are defined as [3]:

$$w_{\Sigma} = a(\nu_l)\,,\ w_{\Delta} = \left.\frac{\partial a(\nu)}{\partial \nu}\right|_{\nu_l} \tag{1}$$

where $a(\nu)$ is the centre phase normalized steering vector in the look direction, N is the number of antenna, ν is the spatial steering frequency, and ν_l is the spatial steering frequency snapshot at time instant l.

2) The spatial processor is an adaptive configuration in which an adaptive beam former is used for the sum and difference weights by applying unity gain constraints in the look direction (target look direction). These weights (sum and difference) may be written in the following form [3]:

$$w_{\Sigma} = \frac{R_x^{-1}v_{\Sigma}}{v_{\Sigma}^H R_x^{-1} v_{\Sigma}}\,,\ w_{\Delta} = \frac{R_x^{-1}v_{\Delta}}{v_{\Delta}^H R_x^{-1} v_{\Delta}} \tag{2}$$

where R_x is the covariance matrix of the input data, ν_{Σ} and ν_{Δ} are the spatial steering frequency for the sum and difference channel respectively and H indicates the Hermitian.

3) The sum and difference outputs are given in terms of the respective processors,

$$z_{\Sigma}(l) = w_{\Sigma}\mathbf{x}(l)\ ,\quad z_{\Delta}(l) = w_{\Delta}\mathbf{x}(l) \tag{3}$$

where $\mathbf{x}(l)$ is the $N \times 1$ spatial snapshot at time instant l.

4) The error voltage The real part of the ratio of difference to sum outputs defined as [2, 3]

$$\varepsilon_v(l) = \Re\left\{\frac{z_{\Delta}(l)}{z_{\Sigma}(l)}\right\} \tag{4}$$

This error voltage conveys purely directional information that must be converted to an angular form via a mapping [2].

5) The standard deviation of the angle error (STDAE) [2] is determined using a target that is injected randomly across the range and angle within the main beam. The corresponding angle error is then averaged over the range and is defined as:

$$\sigma_{\varepsilon_\phi} = \sqrt{E\{\left|\varepsilon_{\phi}\right|^2\}} \tag{5}$$

where $\varepsilon_\phi = \hat{\phi} - \phi$, ϕ is the target angle, and $\hat{\phi}$ is the measured deviated angle from its ideal value due to distortion. When there is no distortion signal (jamming signal) STDAE is near zero and its value will increase due to the existence of the distortion signal.

6)Barrage noise jamming [1, 4] is the most common form of hostile interference. Such interference emanates from a spatially localized source that is temporally uncorrelated from sample to sample as well as from pulse repetition interval to pulse repetition interval. Barrage noise jamming $\boldsymbol{n}_{jam}(t)$ is modelled as the Kronecker product of a white Gaussian $\boldsymbol{n}_j(t)$ noise vector with a spatial steering vector,

$$\boldsymbol{n}_{jam}(t) = \boldsymbol{n}_j(t) \otimes a(v) \tag{6}$$

where the power of each component of $\boldsymbol{n}_j(t)$ is σ_j^2.

III. Empirical Mode Decompostion

A. Classical EMD

EMD is a non-linear technique for analysing and representing non-stationary signals [5-8]. EMD is data-driven and decomposes a time domain signal $x(n)$ into a complete and finite set of adaptive basis functions which are defined as Intrinsic Mode Functions (IMFs), $h^{(i)}(n)$, $1 \le i \le L$. Although these IMFs are not predefined as in the case with the Fourier and the Wavelet Transforms, the IMFs that are extracted are oscillatory and have no DC component, so the signal $x(t)$ can be represented as

$$x(n) = \sum_{i=1}^{L} h^{(i)}(n) + d(n) \tag{7}$$

where $d(n)$ is the residual [5-8].

B. Bivariate EMD

The classical EMD described above can only be applied to real-valued time series. The bivariate EMD is used for complex valued time series [8]. As with the classical EMD, the bivariate EMD is used to separate the more rapidly rotating components from slower ones. The procedure is to define the slowly rotating component as the mean of some envelope. However for complex sequences the envelope is a three-dimensional cylinder that encloses the signal.

C. IMF denoising and thresholding

1) IMF denoising

When the signal $x(n)$ comprises a slowly oscillation (in our case chirp radar signal) superimposed on a highly oscillation signal (in our case high power noise interference), the first IMFs output tend to contain the highly oscillation signal. The concept of denoising is to calculate an estimate of the IMF number at which all previous IMFs may be considered as noise and the subsequent IMFs are considered to contain the useful signal. The IMF denoising technique depends on assuming that the 1st IMF, $h^{(1)}(n)$, captures mostly noise, the noise level $\hat{W}[1]$ is estimated in $x(n)$ by computing [5]

$$\hat{W}[1] = \sum_{n=1}^{N} [h^{(1)}(n)]^2 \tag{8}$$

where N is the number of samples. The noise only IMF energies can be approximated for white Gaussian noise dependence on the energy of the first IMF $h^{(1)}(n)$ from [5]

$$\hat{W}[i] = \frac{\hat{W}[1]}{0.719} \times 2.01^i \tag{9}$$

The threshold level energies $T[i]$ are calculated using the approximated IMF energies in (9) from [5]

$$\log_2(\log_2(\frac{T[i]}{\hat{W}[i]})) = 0.46 \times i - 1.92 \tag{10}$$

Computing the IMFs energies by applying EMD algorithm on $x(n)$ (signal + noise) from [5]

$$W[i] = \sum_{n=1}^{N} [(h^{(i)})(n)]^2 \tag{11}$$

Comparing IMFs energies $W[i]$ with threshold level energies $T[i]$ allows us to determine exactly when the signal energy level crosses the threshold level. Let this occur at $i = k$. The signal $x(n)$ is denoised by reconstruction using only IMFs whose energy exceeds the threshold according to

$$x(n) = \sum_{i=k+1}^{L} h^{(i)}(n) + d(n) \tag{12}$$

2) IMF thresholding

Wavelet thresholding is based on estimating the noise level in each sub band [7]. A similar process can be used in EMD. In EMD direct thresholding (EMD-DT) estimates the noise level in each IMF using a threshold $T_r[i]$ for soft or hard decision using [7]

$$T_r[i] = C\sqrt{W[i]2\ln(N)} \tag{13}$$

where C is a multiplication factor.

Using EMD-DT, the resultant thresholded IMF signals will be exhibit discontinuities. To deal with these discontinuities an adaptive threshold function named EMD interval thresholding (EMD-IT) is employed.

In EMD-IT for any sample interval $\boldsymbol{I}_j^{(i)} = [I_j^{(i)}\ I_{j+1}^{(i)}]$ in $h^{(i)}(n)$ where $h^{(i)}(r_j^{(i)})$ is the single extrema corresponding to this interval, the EMD-IT hard thresholding is defined as [7]

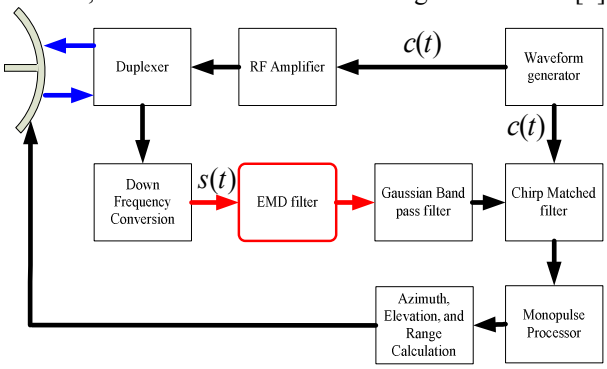

Fig. 1 New structure of the proposed monopulse radar

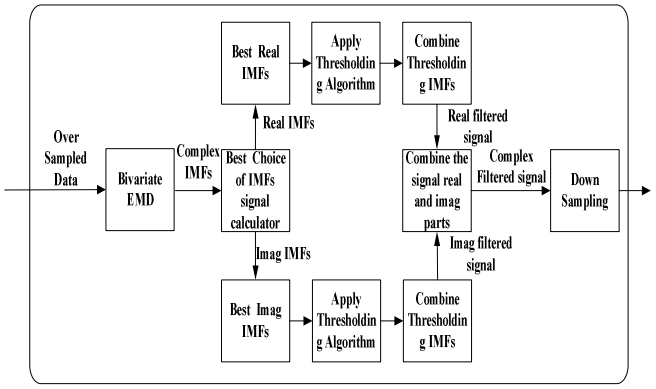

Fig. 2 EMD filter structure

$$h^{(i)}(\boldsymbol{I}_j^{(i)}) = \begin{cases} h^{(i)}(\boldsymbol{I}_j^{(i)}), & \left|h^{(i)}(\boldsymbol{r}_j^{(i)})\right| > T_r[i] \\ 0, & \left|h^{(i)}(\boldsymbol{r}_j^{(i)})\right| \le T_r[i] \end{cases} \tag{14}$$

while the EMD-IT soft thresholding is defined as

$$h^{(i)}(\boldsymbol{I}_j^{(i)}) = \begin{cases} h^{(i)}(\boldsymbol{I}_j^{(i)}) \dfrac{\left|h^{(i)}(\boldsymbol{r}_j^{(i)})\right| - T_r[i]}{\left|h^{(i)}(\boldsymbol{r}_j^{(i)})\right|}, & \left|h^{(i)}(\boldsymbol{r}_j^{(i)})\right| > T_r[i] \\ 0, & \left|h^{(i)}(\boldsymbol{r}_j^{(i)})\right| \le T_r[i] \end{cases} \tag{15}$$

IV. A New Structure Of Monopulse Radar

The proposed EMD based monopulse radar is illustrated in Fig. 1. It comprises a conventional monopulse subsystem along with an additional EMD filter block. A pulse chirp signal $c(t)$ defined in (1) is produced from the waveform generator and is up-converted to the radar carrier frequency, amplified and passed through the duplexer to be transmitted. The down-converted received signal passes through a band limited Gaussian filter. The received signal $s(t)$ may be expressed in the baseband as:

$$s(t) = \begin{cases} [(Ae^{-j2\pi\phi} e^{j\pi(\frac{F_{stop}-F_{start}}{T})(t-T_{start}-\frac{T}{2})^2}).F_d] \times F_\phi & T_{start} < t < T_{start}+T \\ 0 & elsewhere \end{cases} \tag{16}$$

where A is the received signal amplitude, ϕ_o is a random phase shift, and T_{start} is the start time of the returned pulse, passes through a band pass Gaussian filter. The start time T_{start} depend on the target range R_t and is determined from:

$$T_{start} = \frac{2 \times R_t}{c} \tag{17}$$

where c is the speed of light with approximate value 3×10^8. The Doppler shift and delay effect on the target chirp signal is determined by the dot product of the chirp signal by the Doppler vector F_d defined as:

$$F_d = \exp(j2\pi f_d(t - T_{start})) \tag{18}$$

where f_d is the target Doppler frequency.

For the phased array receiving antenna, the antenna phase factor F_ϕ is introduced by

$$F_\phi = \exp(-j2\pi f_c(T_{start} - \boldsymbol{N} \times \Delta t)) \tag{19}$$

where $\boldsymbol{N}$ is a vector represented as $0:N-1$, and Δt is calculated from

$$\Delta t = \frac{D \times \sin\phi_t}{c} \tag{20}$$

where D is the separation between the antenna elements, ϕ_t is the target angle from the antenna boresight.

As seen in Fig. 1 the EMD filter obtains the received radar data $s(t)$ before being passed through the Gaussian band pass filter and then to the chirp matched filter. The EMD filtered matched data supplied to the monopulse processor is used to calculate enhanced target information (due to the added EMD filtering) to direct the antenna towards the target.

The detail construction of the proposed EMD filter is shown in Fig. 2. It starts with over sampled data $s(t)$ (10 times the required sampling frequency of the radar data) because the higher the number of samples, the higher the number of IMFs that are produced using the EMD algorithm [3]. The over sampled complex chirp radar signal is supplied to the bivariate EMD to produce the complex IMFs.

The bivariate EMD complex IMFs outputs are denoised according (8-11). Only IMFs whose energy exceeds the threshold as in (12) are kept. The resultant real and imaginary IMFs after denoising go through two identical paths, one for the real IMFs and one for the imaginary IMFs. The real IMFs passes through the thresholding block which applies EMD-IT using soft thresholding. The resultant thresholded IMFs are combined to produce the real part of the signal (denoised and threshold). The imaginary IMFs are denoised and thresholded in a similar fashion. Finally the real part and imaginary part of the signal are combined to produce the complex filtered signal. The EMD filtered signal is down sampled to the sample frequency used in the radar system to continue data processing. All the output signals from the N EMD filters are then passed to the matched filter and supplied to the monopulse processor as illustrated in Fig. 1 to calculate the target information parameters using (2-5).

V. Simulation Results

The simulated monopulse processor comprises an array of 14 elements spaced 1/3 meters apart. The radar pulse width is 100 microseconds and the pulse repetition interval of 1.6 milliseconds for a 435 MHz carrier. A 200 kHz Gaussian band filters the incoming data returns prior to sampling. The incoming baseband signals are sampled at 1 MHz. Also it is assumed that the radar operating range is 100:200 range bins with a starting window at 865 microseconds and a window duration of 403 microseconds. The target is considered at range bin=150 at angle 32^o from the look direction with target signal to noise ratio (SNR) set to 70 dB with Doppler frequency 150 Hz. A jamming signal with interference noise ratio (INR) set to 75 dB at angle 32^o from the look direction (main beam jamming) and a second at angle 62^o from the look direction (side lobe beam jamming) are introduced. The received signal $s(t)$ is over sampled to 10 MHz (10 times the radar sampling frequency) as described in section IV. The real and imaginary part of the received signal when no jamming signal comprises a chirp signal that starts at bin 150 (target

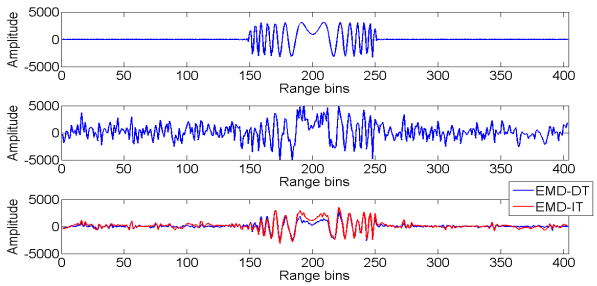

Fig. 3 Real part of the received signal, (a) no jamming, (b) with jamming and no filtering, (c) with jamming and EMD filtering

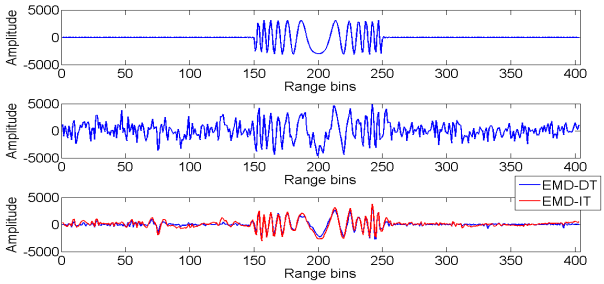

Fig. 4 Imaginary part of the received signal, (a) no jamming, (b) with jamming and no filtering, (c) with jamming and EMD filtering

range) and pulse width of 100 bins (100 msec.) as shown in Fig. 3(a) and Fig. 4(a) respectively. In Fig. 3(b) and Fig. 4(b), the real and imaginary part of the received signal is highly corrupted with the jamming signal. This distortion affects the tracking angle of the tracked target resulting in a probable mistracking outcome. The error voltage is calculated from (4). The complex corrupted received chirp signal due to jamming passes through EMD filter described in section IV. The output filtered signal is shown in Fig. 3(c) and Fig. 4(c). It is clear that from these figures that the jamming interference signal is highly reduced and the enhancement in the signal is significant using the EMD-IT.

The tracking radar system performance is measured by STDAE in (5), the higher the STDAE the less the tracking performance. STDAE is calculated for different target SNRs (from 20-100 dB) for a jamming scenario with interference noise ratio (INR) set to 82 dB with two angles, first at angle 32^o from the look direction (main beam jamming) and second at angle 62^o from the look direction (side lobe beam jamming) are introduced.

In Fig. 5, the STDAE is presented for both jamming scenarios for the conventional monopulse processor. It is clear that for each target SNR the STDAE value decreases in the case of using EMD filtering which indicates an improvement in the tracking performance. For example at target SNR equal 70 dB (vertical red dashed line) the STDAE value decreases from 3.2 to 0.8 in the main lobe jamming and from 0.6 to 0.4 in the side lobe beam jamming. Also the STDAE for the spatial adaptive monopulse processor decreases using EMD filtering as shown in Fig. 6 for main lobe interference and fails for side lobe. For example at target SNR equal 70 dB the STDAE value decreases from 3.5 to 0.3 in the main lobe jamming but it increases at target SNR equal 20 dB from 0.5 to 0.7 in side lobe jamming. It reaches near zero

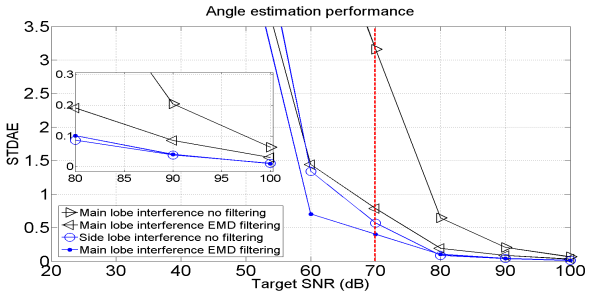

Fig. 5 STDAE for Conventional processor configuration

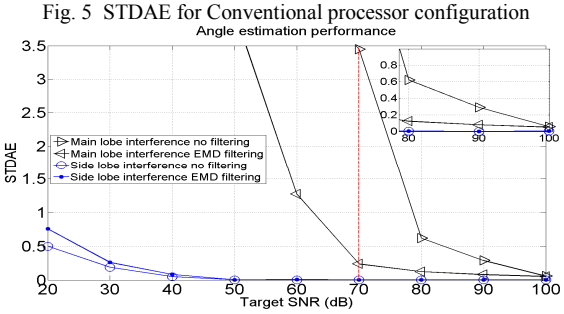

Fig. 6 STDAE for Spatial adaptive processor configuration

(average value 0.003) for side lobe interference with INR equal 53 dB. In Fig. 5 and Fig. 6, the higher SNR the less enhancement is noticed in the STDAE values due to the fact that the target signal power is increased as seen in the zoomed area in both figures.

VI. Conclusion

In this paper a new solution to the distortion problem in the monopulse tracking radar due to high power manmade interference was presented. The distortion resulting from jamming interference appearing in the monopulse main lobe and side lobe has been investigated. The proposed new EMD based monopulse radar system configuration with *N* optimum EMD filters successfully reduces the interference noise signal for the both considered monopulse processors compared to the monopulse radar without filtering. Thus an improvement in the radar tracking ability for different SNR (lower STDAE) is gained by using the suggested EMD filtering technique.

References

[1] D. L. Adamy, *EW 102: a second course in electronic warfare*: Horizon House Publications, Inc., 2004.

[2] Y. Seliktar, "Space- Time Adaptive Monopulse Processing." vol. PhD: Georgia Institute of Technology, 1998.

[3] S. Yaron, B. W. Douglas, and E. J. Holder, "A space/fast-time adaptive monopulse technique." vol. 2006: Hindawi Publishing Corp., pp. 218-218.

[4] M. I. Skolnik, *Radar Handbook-Third edition*: McGraw-Hill, Inc., 2008.

[5] P. Flandrin, P. Goncalves, and G. Rilling, "Detrending and denoising with Empirical Mode Decompositions," in *The 2004 European Signal Processing Conference (EUSIPCO-2004)*, 2004

[6] P. Flandrin, P. Goncalves, and G. Rilling, "EMD Equivalent Filter Banks, from Interpretation to Applications," in *Hilbert-Huang Transform and Its Applications* World Scientific, 2005, pp. pp. 57 -74.

[7] Y. Kopsinis and S. McLaughlin, "Development of EMD-Based Denoising Methods Inspired by Wavelet Thresholding," *Signal Processing, IEEE Transactions on,* vol. 57, pp. 1351-1362, 2009.

[8] G. Rilling, P. Flandrin, P. Gonalves, and J. M. Lilly, "Bivariate Empirical Mode Decomposition," *Signal Processing Letters, IEEE,* vol. 14, pp. 936-939, 2007.